Surface Deposition and Phase Behavior of Oppositely Charged Polyion/Surfactant Ion Complexes. 1. Cationic Guar versus Cationic Hydroxyethylcellulose in Mixtures with Anionic Surfactants

Anna V. Svensson,*,† Lynga Huang,† Eric S. Johnson,‡ Tommy Nylander,† and Lennart Piculell†

Division of Physical Chemistry, Center for Chemistry and Chemical Engineering, Lund University, P.O.B. 124, SE-221 00 Lund, Sweden, and Sharon Woods Technical Center, P&G Beauty & Grooming, 11511 Reed Hartman Highway, Cincinnati, Ohio 45241-2422

ABSTRACT Mixtures of cationic guar (cat-guar) or cationic hydroxyethylcellulose (cat-HEC) with the anionic surfactants sodium dodecyl sulfate or sodium lauryl ether-3 sulfate have been investigated by a wide range of complementary techniques (phase studies, turbidity measurements, dynamic light scattering, gel-swelling experiments, and in situ null ellipsometry), with the following objectives in mind: (1) to establish the relationship between the bulk phase behavior (precipitation and redissolution) of the polyion/surfactant ion complexes and formation/deposition of such complexes at silica surfaces and (2) to obtain molecular interpretations of the large, previously unresolved, quantitative differences between the various investigated mixtures. There were clear similarities, for each studied system, between the bulk phase behavior, gel swelling, and surface deposition on increasing surfactant concentration. This is because all phenomena reflect the polyion/surfactant ion binding isotherm: an initial binding step at a low critical association concentration (cac) of the surfactant and a second more-or-less cooperative binding step beginning at a second cac, the cac(2). The details of the interactions are system-specific, however, and cat-guar/surfactant mixtures generally had larger precipitation regions and gave rise to larger adsorbed amounts on silica compared to mixtures with cat-HEC of a similar charge density. The observed quantitative differences are attributed to a difference in the hydrophobicity of the polyions. For cat-guar, the comparatively weak hydrophobic polyion/surfactant attraction is seen as a very gradual binding commencing at the cac(2) and continuing past the bulk critical micelle concentration of the surfactant, resulting in an unusually large phase-separation region. For cat-HEC, the dissolution of the precipitate takes place at lower surfactant concentrations because of a stronger hydrophobic interaction between the surfactant and the polyion. The results have implications for the successful design of oppositely charged polyelectrolyte/surfactant formulations for surface deposition applications.

KEYWORDS: polyelectrolyte • surfactant • complex • coacervation • adsorption • cationic • guar • hydroxyethylcellulose

INTRODUCTION

Formulations of charged polymers (polyions, PI) and oppositely charged surfactants (surfactant ions, SI) are very common in a number of different applications, such as pharmaceutics (1, 2), personal care products (3) and waste water treatment (4). The strong electrostatic attraction between PI molecules and SI aggregates, both containing multiple charges, induces an associative phase separation of a concentrated phase enriched in both PI and SI from a dilute aqueous phase containing mostly small ions (5, 6). The general behavior of aqueous PI/SI mixtures of opposite charge has been the subject of extensive research (7, 8), and we will here recall some of the main features that are of relevance for the present study. The onset of SI binding to the PI typically occurs at a *critical association concentration (cac)*, which is the surfactant concentration where SI aggregates start to form on the PI (8). When the surfactant concentration is increased beyond the cac, associative phase separation typically occurs. If the PI is sufficiently hydrophobic, a second cooperative binding step may occur at the *hydrophobic* or the *second cac*, *cac(2)* (9, 10). As a result, the complexes will become overcharged by excess bound SI and, in some cases, redissolve (11, 12). This behavior is conveniently summarized in a phase map, showing the bulk phase behavior versus composition of quasi-ternary mixtures of polyelectrolyte, oppositely charged surfactant, and water (11−14).

In many applications, such as hair care and fabric care, the purpose of using formulations based on oppositely charged PI/SI pairs is to obtain deposition of an insoluble PI/SI complex at a solid surface (3, 15). The adsorption of PI/SI

* Corresponding author. Present affiliation: Danish Technological Institute, Taastrup, Denmark. E-mail: anna.svensson@teknologisk.dk. Tel.: +45 72 20 24 77.

Received for review June 2, 2009 and accepted September 23, 2009

† Lund University.

‡ The Procter & Gamble Company.

DOI: 10.1021/am900378b

complexes at surfaces reflects the solution conditions and is affected by factors such as the ionic strength, pH, PI charge density, and bulk concentration. In addition, the charge and hydrophobicity of the surface are important, as is the order of the addition of the components to the dispersion from which the deposition occurs. The rapidly growing literature on the adsorption of oppositely charged PI/SI complexes at solid/liquid interfaces has recently been reviewed (16).

In typical deposition applications, phase separation/deposition is obtained by diluting a single-phase formulation containing an excess of surfactant, where the PI/SI complexes are overcharged and soluble in the bulk. Upon dilution, the bulk concentration of SI decreases, and SI therefore leave the complex in order to satisfy the binding isotherm. Eventually, the net charge of the complex becomes sufficiently low so that phase separation/deposition can occur. While the overall features of this deposition scenario seem well established, there is a poor molecular understanding of the quantitative differences in deposition that result from changing the system components, and this is the focus of the present study, which is the first in a series of papers on the surface deposition of PI/SI complexes. Another aspect, important for applications, is the possibility of tuning or enhancing the deposition at solid surfaces by sequential deposition or deposition−rinsing steps, whereby nonequilibrium or trapped states of the adsorbed layers are accessed (17−22). The challenging topic of history-dependent deposition is outside the scope of the present study but will be addressed in subsequent studies in this series.

Polysaccharides are widely used in industry as deposition agents. They are commonly cationically modified and used in mixtures with anionic surfactant. Especially, cationic guar (cat-guar) (23−26) and cationic hydroxyethylcellulose (cat-HEC) (27−30) have found widespread use in personal care products. It has been observed that cat-guar and cat-HEC perform quantitatively different both in formulations for surface delivery (Procter & Gamble, unpublished results) and in their bulk phase behavior (11, 23), but the reasons have not been understood. The few previous publications concerning the phase behavior of cat-guar in mixtures with anionic surfactant show that the redissolution of cat-guar/surfactant complexes occurs at an unusually large excess of surfactant (11, 23, 24). The surfactant excess required to redissolve the precipitate of cat-HEC/anionic surfactant is much smaller (11, 29−31). The choice of anionic surfactant is also significant for the quantitative behavior. Most studies on cat-HEC and cat-guar have focused on alkyl sulfate surfactants, and particularly sodium dodecyl sulfate (SDS), whereas studies involving the similarly industrially relevant alkyl ether sulfates are much fewer (24, 32).

The present study aims to (1) establish under what conditions complexes of a given PI/SI combination are redissolved by excess surfactant and how this can be related to the properties of the polyion (this is an essential question for the design of formulations for surface delivery) and (2) establish the relationship between the bulk phase behavior and surface deposition. From a formulation perspective, it is important to know, for instance, to what extent the observed turbidity, resulting from a bulk phase separation, can be used as an indicator for surface deposition.

In order to achieve these aims, we have made here a detailed investigation of the relation between the bulk phase behavior of PI/SI complexes, on the one hand, and their deposition at model silica surfaces, on the other hand. We focus especially on the important redissolution behavior. We employ a wide range of techniques, here combined for the first time in a single study. In situ null ellipsometry is used to study the adsorption of the mixtures on hydrophilic and hydrophobic silica. Turbidity measurements are used to investigate the bulk properties at low concentrations (∼0.01 wt %), while phase studies are used to reveal the bulk behavior at high concentrations (0.1−5 wt %). The swelling of cross-linked polysaccharide gel pieces in surfactant solutions is used to study the surfactant binding to the PI without the interference of precipitation (9, 10). Finally, dynamic light scattering (DLS) is used to estimate the size of the dissolved PI/SI complexes.

We have chosen to study industrially relevant PI and SI, that is, cat-guar or cat-HEC, in mixtures with SDS or sodium dodecyl trioxyethylene sulfate, also known as sodium lauryl ether-3 sulfate (SLE3S). Some studies on mixtures of cat-HECs and SDS, using some of the techniques of this study, have been made before, mostly in the Physical Chemistry laboratory at Lund University (9, 29−31, 33, 34). However, for the present purpose of making detailed comparisons, it was essential here to include new and more detailed measurements in a range of cat-HEC samples. We shall find that our multitechnique approach indeed gives new insights, which are valuable in their own right and also allow us to make more general predictions that can be exploited in future studies.

EXPERIMENTAL SECTION

Materials. Guar grafted with (hydroxypropyl)trimethylammonium chloride (cat-guar) was supplied by Hercules Inc. Samples of hydroxyethylcellulose grafted with (hydroxyethyl)-trimethylammonium chloride (cat-HEC) were supplied by Amerchol Corp.: UCARE polymer JR-30M, UCARE polymer LR-30M, and an experimental, low-charge-density, high-molecular-weight (MW) cationic cellulosic polymer. In this paper, these cat-HEC samples are referred to as cat-HEC(1.1), cat-HEC(0.6), and cat-HEC(0.4); see Table 1. Schematic pictures of the repeating units of the polysaccharides are shown in Figure 1.

The polyelectrolytes were purified in order to remove small, water-soluble molecules such as salts and, in the case of cat-guar, also water-insoluble material and proteins. The purification of cat-HEC was made by dialysis with Millipore (MP) water using an Ultrasette Tangential Flow Device from Filtron Technology Corp. A 1 wt % polyelectrolyte solution was prepared and pumped through the device with MP water in the other circuit. The pore size of the filter was 10 K. The dialysis was stopped after 24 h when the outgoing "waste"water had reached low conductivity (< 2 μS/cm). The dialyzed cat-HEC solution was freeze-dried. Industrial-grade guar gum typically contains 4−6% protein and 2.5−5.5% acid-insoluble material originating from the plant seeds from which the guar has been extracted (35). The purification of high MW cat-guar was made here by the following steps: centrifugation, to remove water-insoluble material, followed by precipitation (repeated three times) of the

Table 1. Investigated Cationic Polysaccharides

name	purification procedure	abbreviation	M_W (g/mol)	N content (mequiv/g)
guar (hydroxypropyl)trimethylammonium chloride		unpurified cat-guar	1 800 000[a]	1.0[b]
guar (hydroxypropyl)trimethylammonium chloride	centrifugation + precipitation in isopropyl alcohol	cat-guar	2 000 000[a]	0.6[b]
trimethylammonium hydroxyethylcellulose chloride	dialysis	cat-HEC(0.4)	1 100 000[a]	0.4[b]
trimethylammonium hydroxyethylcellulose chloride	dialysis	cat-HEC(0.6)	1 000 000[a]	0.6[b]
trimethylammonium hydroxyethylcellulose chloride	dialysis	cat-HEC(1.1)	2 000 000[c]	1.1[b]

[a] Weight-average molar mass from GPC-LS. [b] Measured as mequiv of nitrogen/g of polyelectrolyte. [c] From the supplier.

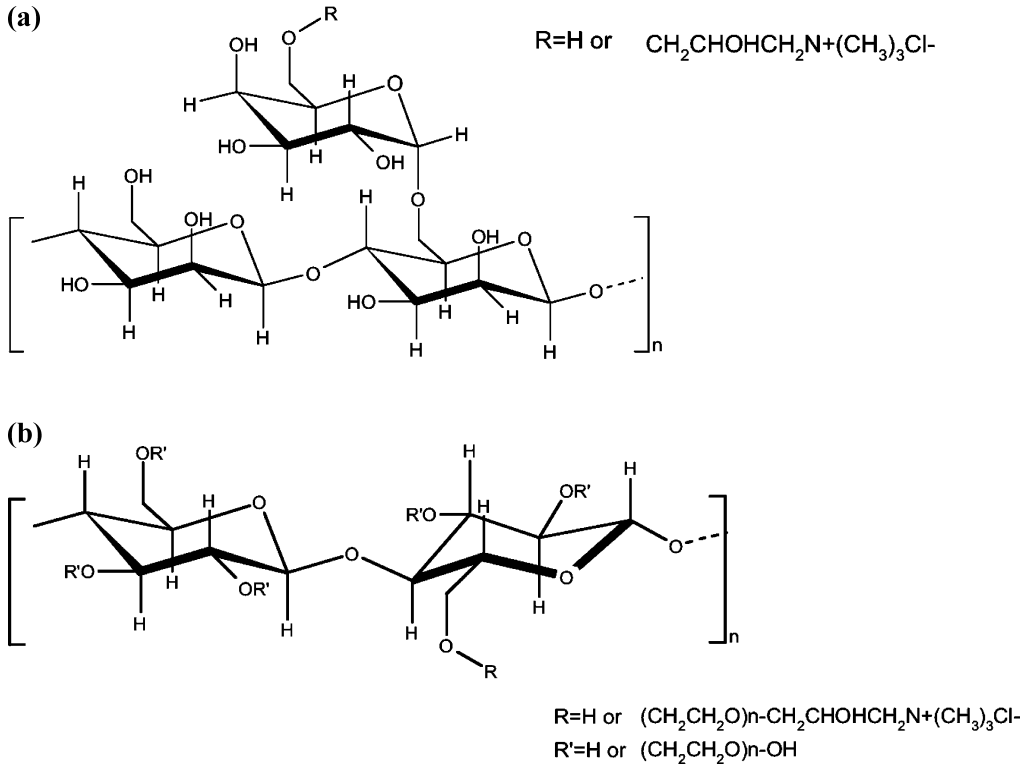

FIGURE 1. Schematic pictures of the repeating units in (a) cat-guar and (b) cat-HEC.

polyelectrolyte in isopropyl alcohol (volume ratio 1:9), and finally drying in a vacuum oven at 40 °C. More details are given in the Supporting Information. The purified cat-guar was completely water-soluble and gave transparent aqueous solutions. The amount of protein residues in the cat-guar samples was estimated by a bicinchoninic acid (BCA) assay, and absorbance measurements at $\lambda = 280$ nm (see the Supporting Information). The purified cat-guar contained 0.6 mequiv of N/g. However, because some protein seemed to remain after purification (see the Supporting Information), 0.6 mequiv/g may be regarded as an upper limit to the true charge density of cat-guar. The complete removal of boron, originally present as borax, during the purification of cat-guar was confirmed by elemental analysis of boron.

Information on the various polysaccharide samples used is collected in Table 1. The cited molecular weights were determined by gel permeation chromatography coupled with light scattering (GPC-LS).

The surfactants were sodium dodecyl sulfate (SDS) from BDH (powder) and sodium lauryl ether-3 sulfate (SLE3S, sodium dodecyl trioxyethylene sulfate) from Procter & Gamble (28 wt % solution, pH 12). The surfactants were used without further purification. In-house characterization at Procter & Gamble revealed that the SLE3S sample was polydisperse, featuring a distribution of 0−8 ethylene oxide groups (with an average of ca. 3) per surfactant molecule and containing, in addition to the dominating C12 fraction, also a significant fraction of longer (mainly C14) alkyl chains. In the gel-swelling experiments, a commercial grade of sodium lauryl (dodecyl) sulfate (SLS) from Procter & Gamble was used (28 wt % solution, pH 12). The commercial grades of SLE3S and SLS contain ca. 0.3 wt % NaCl, 0.1 wt % Na_2SO_4, and 0.7 wt % unsulfated material. The pH was adjusted to neutral with HCl. The weight percentages of the SLE3S and SLS solutions were confirmed by freeze-drying.

Reported critical micelle concentration (cmc) values in water at ambient temperature are 8.1 mM for SDS (36) and 0.8−2.8 mM for SLE3S (24, 37).

In Situ Null Ellipsometry. An automated Rudolph Research thin-film null ellipsometer type 43603-200E was used to measure the adsorbed amount and the thickness of the adsorbed layers in situ. All measurements were performed at a wavelength of 4015 Å, using a xenon lamp with a filter. The substrates used were silicon wafers, which were cut in 12 × 20 mm pieces and thermally oxidized to obtain a silicon oxide layer with a thickness of 300−350 Å. The substrates were cleaned for 5 min in a boiling alkaline bath ($NH_3/H_2O_2/H_2O$) and for 10 min in a boiling acidic bath ($HCl/H_2O_2/H_2O$) as described previously (38). After thorough rinsing with MP water, they were stored in pure ethanol. The hydrophilic silica substrates were dried with nitrogen and plasma-cleaned for 5 min before

measurements. The hydrophilicity of the surfaces was verified by complete wetting by a droplet of water. During preparation hydrophobic surfaces, the washed and plasma-cleaned silica substrates were put in a low-pressure atmosphere of octyldimethylchlorosilane overnight. The substrates were sonicated in (1) ethanol and (2) tetrahydrofuran three times each, followed by thorough rinsing with ethanol and storage in ethanol. The hydrophobic surfaces had a water contact angle of >90°. Each hydrophilic or hydrophobized silica wafer was characterized in the ellipsometer in air and in 1 mM NaCl, which gave information about the thickness and refractive index of the silicon oxide layer and the refractive index of the silicon (38). A hydrophilic silica is negatively charged in water because of the deprotonation of the surface SiOH groups. To reduce air/vapor trapped onto the hydrophobized silica, ethanol was pumped through the cuvette before the 1 mM NaCl solution. The solution in the cuvette was agitated with a magnetic stirrer.

In the adsorption experiments, 0.5 mL of a 1000 ppm polyelectrolyte solution was added to the cuvette previously filled with 4.5 mL of 1 mM NaCl of pH 6.5, yielding a final polyelectrolyte concentration in the cuvette of 100 ppm. Known small amounts of 10, 100, or 500 mM surfactant solutions were progressively added to obtain the desired surfactant concentrations. The adsorption after each addition was allowed to reach a steady state, which took approximately 2000−3000 s. This surfactant titration method is an efficient protocol for measuring the adsorption from PI/SI mixtures covering a wide range of surfactant concentrations in a single experiment.

The raw data of the ellipsometry measurement are the so-called ellipsometric angles, Ψ and Δ, which correspond to the relative amplitude change and the relative phase shift, respectively, upon reflection of polarized light at an interface. The angles are evaluated using a four-layer optical model, assuming isotropic layers and planar interfaces, to obtain the thickness and refractive index of the adsorbed layer by means of an iterative procedure (38). The adsorbed amount is then calculated by using the values of the thickness and the refractive index of the layer, according to

$$\Gamma = \frac{d_f(n_f - n_0)}{dn/dc} \quad (1)$$

Here Γ is the mass per surface area, d_f the thickness of the adsorbed film, n_f the refractive index of the adsorbed film, n_0 the refractive index of the bulk solution, and dn/dc the refractive index increment as a function of the bulk concentration. The dn/dc values of the polyelectrolytes were measured by GPC-LS as 0.153 mL/g for cat-guar and 0.129 mL/g for cat-HEC(0.6). The dn/dc value of SDS has been measured as 0.147 mL/g in an earlier work (34). Because one cannot resolve the relative contributions to the adsorbed layer from PI and SI by ellipsometry at a single wavelength, we used a single approximate dn/dc value of 0.15 mL/g for all PI, SI, and mixtures thereof in the present study.

Duplicate or multiple measurements were made in some instances to test for reproducibility. Four separate measurements on cat-guar gave 0.7−0.8 mg/m^2 in adsorbed amount and 120−250 Å in thickness (mean value 190 Å). Seven separate measurements of cat-HEC(0.6) on hydrophilic silica gave plateau values ranging from 0.5 to 1.2 mg/m^2 in adsorbed amount (mean value 0.9 mg/m^2) and between 50 and 130 Å in thickness (mean value 80 Å). Duplicate titrations with SDS were made for cat-guar and cat-HEC(0.6), and the differences obtained are shown as error bars in Figures 4 and 5.

UV−Vis Spectrophotometry. The turbidity of the bulk solutions was determined by absorbance measurements in the visible light region (λ = 500 nm). PS cuvettes with a path length of 1 cm were used. The conditions in the cuvette during the turbidity measurements were similar to those in the ellipsometry measurements, with stepwise addition of surfactant to a polyelectrolyte solution and stirring between the measurements. The absorbance was measured 5 min after the surfactant addition and repeated after 10, 20, and 30 min of stirring.

Phase Studies. Pseudoternary phase maps were obtained by the direct mixing of polyelectrolyte, surfactant, and MP water. Appropriate amounts of dry polyelectrolyte and dry surfactant (or surfactant solution) were weighed in a glass tube. The mixture was shaken lightly using a Vortex table mixer. Water was added to the mixture, and the tube was sealed with a cap. The total weight of the sample was 1 or 2 g. The sample was shaken by hand and by a Vortex mixer. It was put on a tilting plate for 24 h, or longer if the sample was not yet homogeneous. Turbid samples were centrifuged at 1200g for 20 min to see if the phases could be separated. The procedure was repeated until the appearance of the sample did not change with time. Each phase map was based on approximately 30 samples evaluated at room temperature (20 °C).

DLS. The setup used for DLS of the polyelectrolyte/surfactant mixtures was an ALV/DLS/SLS-5000F, CGF-8F-based compact goniometer system from ALV-GmbH, Langen, Germany. The light source is a continuous-wave, diode-pumped Nd:YAG solid-state Compass-DPSS laser with a symmetrizer from Coherent, Inc., Santa Clara, CA. It operates at 532 nm with a fixed output power of 400 mW. The laser intensity can be modulated by an external compensated attenuator from Newport Corp., Irvine, CA. The instrumental settings are described elsewhere (39). The measuring temperature was set to room temperature. The scattering angle was fixed at 90°.

In the DLS measurements, the time-correlation function (auto or pseudo-cross) of the scattered intensity is constructed using two correlators of 320 total exponentially spaced channels. The normalized intensity correlation function $g^{(2)}(t)$ is related to the normalized time-correlation function of the electric field $g^{(1)}(t)$ by Siegert's relation $g^{(2)}(t) - 1 = \beta[g^{(1)}(t)]$ (2), where t is the lag time and β ($\leq$1) is a coherence factor that accounts for the deviation from the ideal correlation and the experimental geometry. For polydisperse particles or for different modes of motion field, $g^{(1)}(t)$ may be described by

$$g^{(1)}(t) = \int_0^\infty \tau A(\tau) \exp(-t/\tau)\, d \ln \tau \quad (2)$$

where τ is the relaxation time and $A(\tau)$ is the relaxation time distribution. The DLS data were analyzed by regularized inverse Laplace transformation to obtain the relaxation time distribution using the algorithm included in the ALV software. The results are shown as relaxation time distributions, that is, $\tau A(\tau)$, as a function of log(τ/ms), which we have normalized with the maximum peak height.

In the limit of small scattering vectors (q), the apparent translational diffusion coefficient (D_{app}) at finite concentration can be calculated from the relaxation rate (G), which is obtained from the first moment of the translational mode in the relaxation time distribution

$$D_{app} = \left(\frac{G}{q^2}\right)_{q \to 0} \quad (3)$$

Here G = 1/τ and q is the magnitude of the scattering vector [$q = 4\pi n_0 \sin(\theta/2)/\lambda$, where n_0 is the refractive index of water, λ is the incident wavelength, and θ is the scattering angle]. From the apparent translational diffusion coefficient, we obtained the apparent hydrodynamic radius through the Stokes−Einstein relationship as

$$R_H^{app} = \frac{kT}{6\pi\eta_0 D_{app}} \quad (4)$$

Here k is Boltzmann's constant, T is the absolute temperature, and η_0 is the viscosity of water.

The samples for the DLS measurements were prepared as follows. The solvent, 1 mM NaCl, was filtered through a 0.1 μm filter. Appropriate amounts of polyelectrolyte, surfactant, and solvent were weighed in a glass container and sealed with a cap. The sample was shaken by hand and by a Vortex mixer. It was put on a tilting plate for 24 h, or longer if the sample was not yet homogeneous. The sample was centrifuged at 3000 rpm for 1 h. The top part of the sample was transferred with a syringe to the glass tube for the DLS measurement.

Gel-Swelling Experiments. The polyelectrolytes used in the preparation of the gel pieces were of comparatively low-MW grades in order to obtain a low viscosity in the synthesis batches. A low-MW cat-guar from Hercules Inc. and a UCARE polymer LR-400 from Amerchol Corp. were used. Both polyelectrolytes were purified by dialysis with MP water; see the description in the Materials section. The cat-guar was first centrifuged at 20 000*g* for 2 h. The charge densities of the dialyzed PI were estimated from the nitrogen content, and the MW was measured by GPC-LS: cat-guar contained 0.5 mequiv of N/g with a M_W of 410 000 g/mol and cat-HEC contained 0.6 mequiv of N/g with a M_W of 430 000 g/mol. The cross-linker used in the gel synthesis was ethylene glycol diglycidyl ether (EGDE; 50 wt % solution) from Sigma-Aldrich. Potassium *tert*-butoxide (K-ButO) from Sigma-Aldrich was used as the initiator. Polyelectrolyte solutions of 3 wt % were prepared. The amount of added EGDE corresponded to a molar ratio of epoxy groups on the cross-linker versus primary hydroxyl groups on the polyion of 2:1. The pH was increased by adding K-ButO before adding EGDE. C_{12}TAB (50 mM) was added to the polyelectrolyte solutions to prevent the cationic gels from sticking to the anionic glass capillaries. Open capillaries (Ø = 1.4 mm) were put in the polyelectrolyte solutions as cylindrical molds. The PI were chemically cross-linked at 60 °C for 24 h. After successful gelation, the gels were ejected by pushing air through the capillaries with a syringe. The gel strings were cut into 2 mm pieces and left to equilibrate in MP water for 1 week to remove unreacted chemicals. The water was renewed every 24 h. The gel synthesis procedure was based on the work of Sjöström and Piculell (9) and Rodriguez et al. (1).

The washed gels were put in beakers with 5 mL of surfactant solutions (SLS and SLE3S) of different concentrations. The gels were left to equilibrate for 1 week before studying the swelling. The diameter of the gel was measured by a video camera, calibrated with a 0.1 mm scale, and recalculated from the camera pixels to millimeters. The swelling was calculated as $(d/d_0)^3/c_0$ where d_0 is the inner diameter of the capillary molds, d is the diameter of the gel 1 week after immersion in a surfactant solution, and c_0 (g/mL) is the polyelectrolyte concentration in the polyelectrolyte mixture at the start. The swelling is given as Vm^{-1} (mL/g), indicating the amount of absorbed water per gram of dry polyelectrolyte.

RESULTS

Dilute Solution Behavior of the PI. Figure 2 compares the relaxation time distributions from DLS measurements of cat-guar and cat-HEC(0.6) in solutions containing 10 mM NaCl to reduce the polyelectrolyte effect. Very similar distributions were obtained for both polysaccharides in 100 mM NaCl (not shown). The distributions were wide for cat-guar and appeared to be bimodal. cat-HEC gave narrower relaxation time distributions, with a single peak

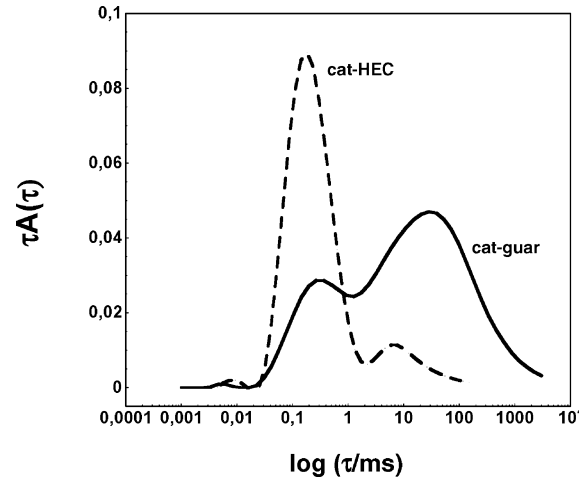

FIGURE 2. Relaxation time distributions at $\theta = 90°$ for 0.1 wt % cat-guar (full line) and cat-HEC(0.6) (dashed line), respectively, in 10 mM NaCl.

corresponding to an apparent hydrodynamic radius of 38 nm in 10 mM NaCl or 49 nm in 100 mM NaCl.

Adsorption of the PI Alone. Representative data for the time-dependent adsorption of cat-guar and cat-HEC(0.6) on hydrophilic and hydrophobic surfaces are shown in Figure 3. Data for the unpurified cat-guar were also obtained and are available as Supporting Information. The initial adsorption of the PI on the hydrophilic (anionic) silica was fast, followed by a slow increase in the adsorbed amount for cat-guar while cat-HEC reached a plateau value much more rapidly. At long times, a slightly higher adsorbed amount was observed for cat-guar than for cat-HEC. The polyion adsorption kinetics on hydrophobized silica was also fast, but on this surface, cat-guar gave a significantly lower adsorbed amount than cat-HEC. The adsorbed amount after 1.5 h was 0.7 mg/m^2 for cat-HEC and 0.4 mg/m^2 for cat-guar. The results for cat-HEC shown in Figure 3 are very similar to those previously reported for the time-dependent adsorption of cat-HEC of lower molecular weight on hydrophilic and hydrophobized silica (29, 30).

Adsorption from cat-guar/SDS Mixtures. The adsorption on hydrophilic silica from cat-guar/surfactant mixtures was investigated in titration experiments, where surfactant was added stepwise to the ellipsometer cuvette initially containing only cat-guar in 1 mM NaCl; see the Experimental Section for details. The steady-state results after each consecutive addition are shown in Figure 4. Upon stepwise increase of the surfactant in the presence of the cat-guar in solution, there was an increase in the adsorbed amount and layer thickness beginning at around 0.1 mM SDS. The adsorbed amount reached a maximum value, which indicates that not only SI but also additional PI were deposited from the bulk when surfactant was added in the cuvette. This follows because the mass of a dodecyl sulfate ion is only 16% of the mass per nitrogen of cat-guar. The maximum adsorbed amount, which appeared at ca. 5 mM SDS, was ca. 3.5 mg/m^2. The above maximum desorption of the complexes, seen as a decrease in the adsorbed amount, occurred together with a swelling of the remaining

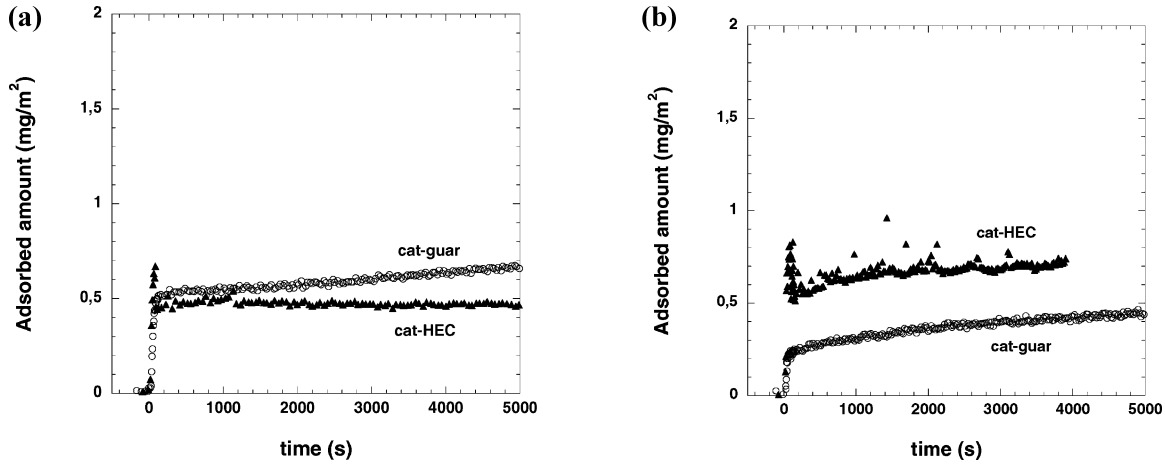

FIGURE 3. Adsorption from 100 ppm polyelectrolyte solutions as a function of time: (a) hydrophilic silica; (b) hydrophobized silica. The solutions were injected at $t = 0$. cat-guar = circles, and cat-HEC(0.6) = triangles.

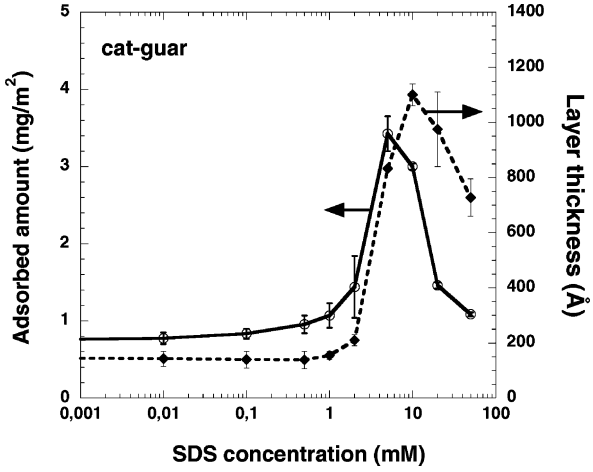

FIGURE 4. Adsorption from cat-guar/SDS solutions at hydrophilic silica as a function of the SDS concentration showing the adsorbed amount (full line, left axis) and thickness (dashed line, right axis) of the adsorbed layer. The polyelectrolyte concentration was 100 ppm, and SDS was added in steps.

layer progressively over a broad range of SDS concentrations. Both processes are expected consequences of the binding of excess surfactant to the PI/SI complexes. The swollen layers had a maximum thickness of 110 nm and decreased to 70 nm at the highest SDS concentration, which was 50 mM.

Adsorption from cat-HEC/SDS Mixtures. cat-HECs of three different cationic charge densities, in a range covering that of cat-guar, were investigated for comparison. Parts a and b of Figure 5 show the adsorbed amounts and the layer thicknesses of cat-HECs on hydrophilic silica, as a function of the increased concentration of SDS. The adsorbed amount without added surfactant decreased with increasing charge density of cat-HEC and was 1.4 mg/m^2 for cat-HEC(0.4), 1.0 mg/m^2 for cat-HEC(0.6), and 0.8 mg/m^2 for cat-HEC(1.1). Upon the addition of SDS, variations in the adsorbed amount and layer thickness similar to those for cat-guar were observed, but there were quantitative variations with differences in the charge density. The position of the maximum in the adsorbed amount shifted to lower SDS concentrations, from 5 to 2 mM SDS, with increasing cat-HEC charge density. (N.B. The adsorbed amount at 2 mM SDS was not measurable for cat-HEC(1.1) because the phase separation in this particular mixture gave rise to a too high turbidity.) We note that the width of the peak in the adsorbed amount, that is, the SDS concentration interval corresponding to enhanced adsorption, was much narrower for all cat-

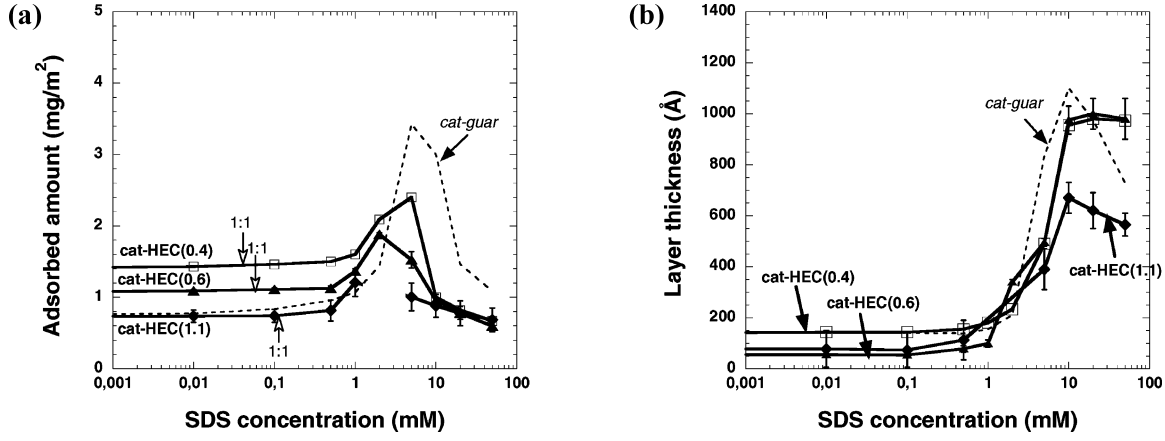

FIGURE 5. Adsorption from cat-HEC/SDS solutions at hydrophilic silica as a function of the SDS concentration showing the (a) adsorbed amount and (b) thickness of the adsorbed layer. cat-HEC(0.4) = squares, cat-HEC(0.6) = triangles, and cat-HEC(1.1) = diamonds. The polyelectrolyte concentration was 100 ppm, and SDS was added in steps. The results for cat-guar from Figure 4 are included for comparison (dotted line).

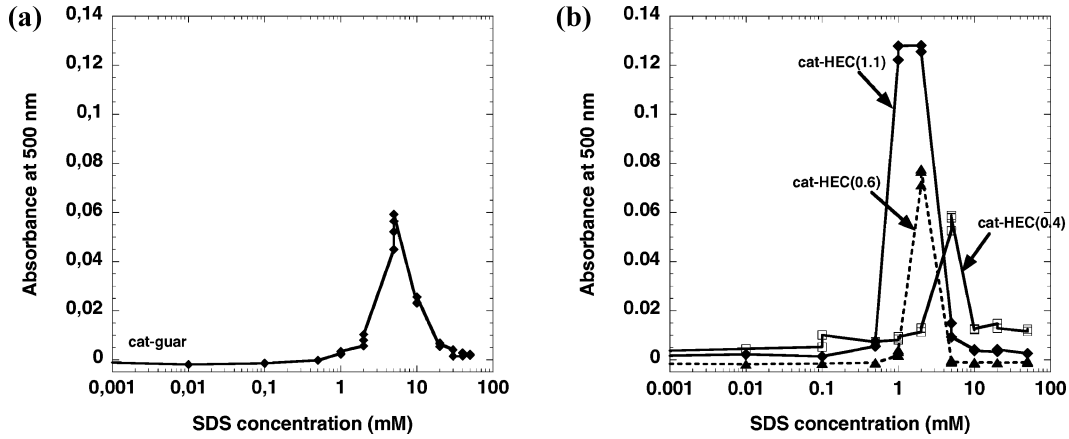

FIGURE 6. Turbidities in 100 ppm polyelectrolyte solutions as functions of added surfactant for (a) cat-guar/SDS and (b) cat-HEC/SDS.

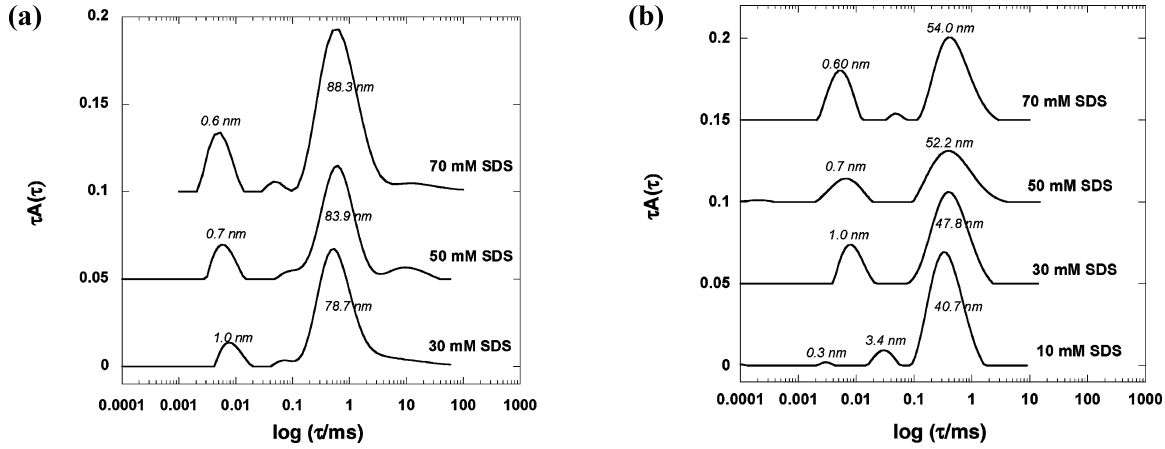

FIGURE 7. Relaxation time distributions at $\theta = 90°$ in mixtures of 100 ppm polyelectrolyte/x mM SDS (x =10, 30, 50, and 70) for (a) purified cat-guar and (b) cat-HEC(0.6). Apparent hydrodynamic radii (see the text) are indicated.

HECs compared to cat-guar; the results for cat-guar from Figure 4 are included for comparison.

Turbidity Measurements in the Bulk. Figure 6 shows the turbidity in the bulk for the various combinations of polyion and SDS during measurements made under the same conditions as those in the ellipsometer, i.e., during the stepwise addition of surfactant to a 100 ppm polyelectrolyte solution. In all cases, a peak in the turbidity was seen, reflecting an initial precipitation of a PI/SI complex followed by a progressive redissolution of the complex by excess surfactant. The complete redissolution of the complex was observed as a low and constant level of turbidity at high surfactant concentrations. A maximum in the turbidity of the cat-guar/SDS bulk solutions occurred at 5 mM SDS (see Figure 6a), which coincided with the adsorption maximum shown in Figure 4. We note that the complete redissolution of the cat-guar/SDS complexes required quite high SDS concentrations, on the order of 30 mM SDS.

The turbidities of the various cat-HEC/SDS mixtures (Figure 6b) reached maxima at 1, 2, and 5 mM SDS, which coincided with the adsorption maxima observed in Figure 5a. The highest turbidity was observed for cat-HEC(1.1). The turbidity had decreased to roughly the initial level again at 5 or 10 mM SDS, depending on the polyion charge density. We note that for all of the cat-HEC samples, in contrast to the cat-guar sample, a complete redissolution of the precipitates occurred at a free-surfactant concentration below or close to the cmc of SDS (ca. 8 mM).

Experiments on Unpurified cat-guar. When cat-guar is used in applied contexts, it is not necessarily purified as in our study. One may thus ask if the surface adsorption and turbidity results for unpurified cat-guar differ markedly from those results shown above. For this reason, we made measurements analogous to those shown in Figures 3–6 also on unpurified cat-guar and on cat-guar purified by centrifugation only. The detailed results are available in the Supporting Information. The most significant effect of the impurities that we observed was an additional slow adsorption process in cat-guar in the absence of surfactant, especially strong on the hydrophobic surface. However, SDS titration experiments as in Figures 4–6 showed very similar results for unpurified and purified cat-guar, except for a slight additional adsorption from the unpurified samples at low surfactant concentrations.

Size of Dissolved PI/SI Complexes. Figure 7 shows the relaxation time distributions from mixtures of cat-guar/SDS and cat-HEC(0.6)/SDS at surfactant concentrations where the complexes were redissolved. The plots feature two peaks, corresponding to fast and slow modes, that can be ascribed to SDS micelles and soluble PI/SI complexes, respectively. The apparent hydrodynamic radii obtained

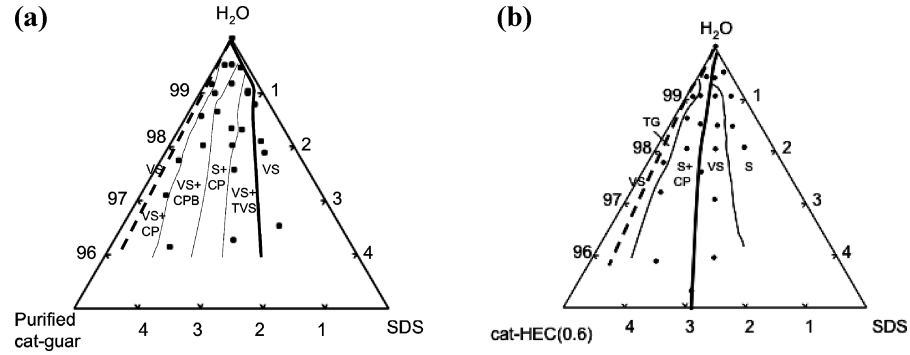

FIGURE 8. Pseudoternary phase maps of aqueous mixtures (in wt %) of SDS with (a) purified cat-guar and (b) cat-HEC(0.6). Thick lines show phase boundaries between one- and two-phase regions. Two-phase samples are characterized as, for example, "S + CP" [S = clear solution, VS = viscous clear solution, TVS = turbid viscous solution, TG = turbid gel, F = fluffy flocs, DP = dispersed precipitate, CP = compact precipitate (a lump), and CPB = compact precipitate with birefringent traces].

from the different modes using the Stokes–Einstein relationship (see the Experimental Section) are indicated in the figures. The cat-guar/SDS complexes were the largest with a radius of ca. 80 nm, while the cat-HEC/SDS complexes had an apparent hydrodynamic radius of ca. 40 nm. For both PI, there was a shift of the slow modes to longer relaxation times with increasing SDS concentration, which could suggest an increase in the size of the complexes. We note that the dominating peak seen in the bimodal distribution for cat-guar alone in Figure 2 corresponding to much larger objects is absent in Figure 7a. Most likely, the additional peak from the surfactant-free cat-guar solution therefore corresponds to polyion aggregates that could be dissolved by surfactant.

Phase Behavior of cat-guar/Surfactant and cat-HEC/Surfactant Mixtures. Pseudoternary phase diagrams for the various polyelectrolyte/surfactant mixtures were constructed to explore the precipitation behavior at polyelectrolyte concentrations much higher than those of the turbidity measurements. Figure 8a shows the diagram for mixtures of cat-guar, SDS, and water. The phase map contains distinct one- and two-phase regions. The binary mixtures of cat-guar and water were transparent because cat-guar was completely soluble in water. The two-phase region contained samples featuring a clear solution in equilibrium with either a compact precipitate or, at higher surfactant/polyelectrolyte ratios, a dispersed precipitate. The redissolution phase boundary, which limits the two-phase region at high surfactant concentrations, is approximately a straight line with a finite intercept on the water–SDS axis. Assuming that this intercept represents the (constant) concentration of free surfactant at redissolution (this assumption is discussed further in the Supporting Information), we can obtain an estimate of the stoichiometry of the redissolved PI/SI complex from the slope of the redissolution boundary (40). We thus obtain a ratio of surfactant to polyelectrolyte at a dissolution of 1.5:1 (S:P weight ratio) or 13:1 (SI:PI charge ratio); see Table 2.

Figure 8b shows the phase map of mixtures of cat-HEC(0.6), SDS, and water. Here, one-phase regions appeared at small excesses of either PI or SI. For cat-HEC(0.6) and SDS, the surfactant/polyelectrolyte ratio at redissolution was 0.8:1 (weight ratio) or 4:1 (charge ratio). The phase maps of cat-HEC(0.4) and cat-HEC(1.1) with SDS (not shown) had appearances similar to that of the diagram of cat-HEC(0.6), with a small two-phase region with a compact precipitate in a clear solution. Table 2 collects the surfactant/polyelectrolyte ratios where the precipitates dissolve. The weight ratio was found to be 0.8:1 for all cat-HEC/SDS systems. Hence, the level of bound surfactant in the complex at redissolution was the same regardless of the cat-HEC charge density. A similar finding has been made previously for cat-guars with a range of charge densities (23).

Table 2. SI/PI Ratios at Dissolution of the Polyion-SDS Complexes (See the Text)

polyion	S:P weight ratio	SI:PI charge ratio
purified cat-guar	1.5:1	13:1
cat-HEC(0.4)	0.7:1	6:1
cat-HEC(0.6)	0.8:1	4:1
cat-HEC(1.1)	0.8:1	2:1

Surfactant Binding Monitored by Gel Swelling. Turbidity measurements and phase maps show where the onset of precipitation and the complete redissolution occur, but they are insensitive to any variation in the binding of the surfactant to the polyion that may occur inside the one-phase regions, that is, prior to precipitation or after complete redissolution. A covalently cross-linked polyelectrolyte gel piece will swell in water because of the electrostatic repulsion between the charges on the polyion and, more importantly, the osmotic pressure exerted by the small counterions in the gel (9, 10). Through immersion of gel pieces in surfactant solutions of increasing concentrations, the onset of surfactant binding, i.e., the cac, is manifested as an onset of shrinking of the gel when bound surfactant aggregates start to gradually neutralize the charges on the polyion. Figure 9 compares the degree of swelling of cross-linked cat-guar (0.5 mequiv/g) and cross-linked cat-HEC (0.6 mequiv/g) immersed in increasing concentrations of SDS. The gels started to shrink in the intervals 0.01–0.05 mM SDS for cat-HEC and 0.05–0.1 mM SDS for cat-guar. Thus, the corresponding cac's are located in these concentration intervals. The gels were fully collapsed when neutral PI/SI complexes had formed. The process of "recharging" the complex by excess surfactant started at the cac(2) and gave rise to a reswelling of the gel driven by the osmotic pressure from the counterions of the excess surfactant (10). This

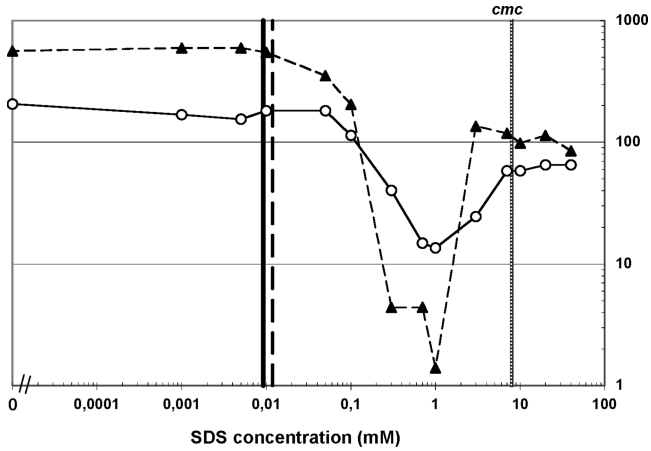

FIGURE 9. Degree of swelling of gels of cross-linked cat-guar (circles) or cross-linked cat-HEC(0.6) (triangles) immersed in solutions containing increasing concentrations of SDS. Vertical lines mark the points of SI/PI charge equivalence for the systems (black line, cat-guar gel; dashed line, cat-HEC gel) and the cmc of the surfactant (gray line).

process corresponds to the redissolution process of the precipitate in the bulk or at the surface (9). The binding of excess SDS started at approximately 1 mM SDS for both cat-guar and cat-HEC gels. However, there was a clear difference between the reswelling processes. The volume of the cat-HEC gel increased sharply and reached a plateau value at 3 mM SDS, indicating that the polyion was saturated with SDS at this point, significantly below the surfactant cmc. The cat-guar gel, by contrast, reswelled to a much lesser extent and only gradually. In fact, the swelling continued beyond the surfactant cmc and never seemed to reach a true plateau in the investigated surfactant concentration range.

Mixtures with SLE3S. Ellipsometry, turbidity, phase separation, and gel-swelling experiments, as reported above for the mixtures with SDS, were also performed for cat-guar and cat-HEC(0.6) in mixtures with SLE3S. The data obtained, which are available in the Supporting Information, reproduced all of the trends regarding the differences between cat-guar and cat-HEC(0.6) in their interactions with anionic surfactant that we have found above for the mixtures with SDS. However, because the cmc of SLE3S is much lower than the cmc of SDS, the cac's were also shifted to lower concentrations in the mixtures with SLE3S. Another difference was that the regions of phase separation at high overall concentrations, seen in the phase maps, were much wider for SLE3S. The latter feature, which we attribute to surfactant polydispersity, is also discussed in the Supporting Information.

DISCUSSION

Consistent Picture of PI/SI Interactions in the Bulk and at Surfaces. Before discussing the specifics of different substances and mixtures, we note that for each system the various methods employed give a consistent picture of the interactions between the polyion and the surfactant, both in the bulk and in the adsorbed layer at hydrophilic silica. It is particularly interesting, and useful, to note that the overall shapes of the adsorption and turbidity curves are generally very similar. For a given PI/SI combination, the turbidity and adsorption peaks show, within the resolution of our experiments, the same surfactant concentrations at the onset of the increase, at the maximum, and at the final leveling off at high surfactant concentrations. This similarity is not surprising because both peaks reflect the surfactant binding isotherm. Therefore, a simple turbidity measurement can serve as a guideline for the position and width of the adsorption peak for a PI/SI pair, that is, the surfactant concentrations at the beginning, maximum, and end of the adsorption peak obtained with increasing surfactant concentration. We note, however, that there is not a similar correspondence between the observed *magnitudes* of the turbidity and adsorption peaks. A strong maximum turbidity in the bulk does not necessarily imply a large maximum surface adsorption. For the cat-HEC systems and hydrophilic surfaces studied here, the reverse is actually the case, as is evident by comparison of the results in Figures 5a and 6b. The highest adsorbed amount at the maximum was obtained for the cat-HEC(0.4)/SDS combination, which showed the lowest maximum turbidity.

When comparing our various results for dilute polyion systems, we note that in the turbidity, ellipsometry, light-scattering, and gel-swelling experiments the amount of free surfactant was vastly in excess of the amount of polyion-bound surfactant at least in the redissolution region above the cac(2), which is of special interest here. In the gel-swelling experiments, the total number of polyion charges per total volume of the swelling solution was 0.01 mM (see Figure 9), 1 or 2 (depending on the surfactant) orders of magnitude below the surfactant concentration at the cac(2). In the turbidity, ellipsometry, and light-scattering experiments, the polyelectrolyte concentration was 100 ppm, corresponding to 0.04−0.1 mM of charged groups, depending on the polyion. Complete redissolution in the latter experiments occurred at lower surfactant concentrations for cat-HEC than for cat-guar, and from the estimated S:P weight ratio at redissolution, 0.8:1 for cat-HEC/SDS (Table 2), we obtain roughly 80 ppm of bound SDS at redissolution of 100 ppm cat-HEC. This corresponds to 0.3 mM of bound SDS, which is negligible compared to the total surfactant concentration of 5−10 mM at redissolution (see Figure 6b). Thus, we may assume that the concentration of free surfactant was essentially equal to the total surfactant concentration at and above the cac(2) in the dilute solution experiments. This makes it possible for us to directly compare the characteristic free-surfactant concentrations at the cac(2) and at redissolution between the different experiments.

At high surfactant concentrations, the light-scattering measurements in the bulk indicate that the PI/SI complexes consist of individual PI chains decorated with bound surfactant micelles. This follows from the sizes of the complexes. We note that under the same conditions the thickness of the adsorbed layer at hydrophilic silica is of the same order of magnitude (ca. 100 nm) as twice the hydrodynamic radius of the complex in the bulk. This suggests that there remains roughly a monolayer of surfactant-swollen PI coils adsorbed

at the surface at a large excess of added surfactant. We may check this interpretation further by a rough estimate of the implied surface coverage. Let us consider a surface completely covered by a two-dimensional layer of adsorbed cat-HEC(0.6)/SDS complexes, each containing one polyion. We assume that each complex occupies an area equal to that of a circle with a 50 nm radius (cf. the measured hydrodynamic radii in Figure 7b); this corresponds to the assumption of an overlap concentration of complexes in the monolayer. With a molecular weight of 10^6 for cat-HEC(0.6), this leads to an adsorbed amount of 0.2 mg/m^2 of cat-HEC(0.6). To this, we have to add the surfactant bound to the polyion. As a reasonable estimate of the composition of the complex, we may use the bulk S:P weight ratio 0.8:1 at redissolution obtained from the phase studies (see Table 2), yielding a total adsorbed amount in the range 0.3−0.4 mg/m^2 at high surfactant concentrations. This amount corresponds to roughly half of the measured surface coverage (see Figure 5a). An exact numerical agreement should not be expected but could be obtained by assuming only a slightly smaller (by a factor of 0.7) effective radius of an adsorbed complex, corresponding to a slight interpenetration or deformation of the complexes. We thus conclude that our calculation agrees with the notion of a layer of densely packed swollen complexes at high surfactant concentrations.

We note in this context that Zimin et al. recently studied both the bulk dimensions of cat-HEC/SDS complexes by DLS and the adsorption of such complexes to mica and hydrophobized silica surfaces by atomic force microscopy (41). However, their results are not directly comparable to ours because their mixtures were limited to low SDS concentrations (3.5 mM or less). Moreover, the history of deposition was different in the experiments of Zimin et al. (41). They exposed fresh surfaces to mixtures of fixed compositions as opposed to, as in our protocol, sequentially adding SDS to a solution in contact with a surface that had been "primed" with an adsorbed polyion layer. Previous experiments in our laboratory have shown that experiments in which a premixed PI/SI solution is contacted with a fresh surface for each surfactant concentration typically give lower adsorbed amounts, especially at high surfactant concentrations (29, 30).

Adsorption Reflecting Polyion Hydrophobicity and Charge Density. The time-dependent adsorption of the polyion alone, in the absence of surfactant, agrees with the previous results for similar systems (29, 30). Here we will only note some quantitative trends of particular relevance in the present context. The measurements on different cat-HECs showed an increase in the adsorbed amount with decreasing charge density (Figure 5a). This is expected because a highly charged polyion adsorbs flatly to the surface (42), whereas a lowly charged polyion will also form loops and tails, resulting in a thicker layer. Anthony et al. showed, by surface force measurements on mica surfaces with adsorbed cat-guar layers, that increasing the polyion charge density resulted in a more compact cat-guar layer (23).

Roughly equal amounts of cat-HEC(0.6) and cat-guar adsorbed at hydrophilic silica surfaces; see Figure 3. However, more of cat-HEC(0.6) than of cat-guar adsorbed to a hydrophobic surface. We suggest that the adsorption at hydrophobized silica can be used to detect differences in hydrophobicity between otherwise comparable PI. Thus, the results in Figure 3 indicate that cat-HEC has a more hydrophobic character than cat-guar.

Polyion Charge Density Affecting the Interaction with Surfactant. The results of the adsorption and turbidity measurements of cat-HECs with different charge densities in mixtures with SDS showed that the charge density is an important parameter; see Figure 5. The lowest adsorbed amount was obtained for the complexes with the most highly charged cat-HEC(1.1), which follows the trend seen for the adsorption of the polyion alone (see above). Moreover, the positions of the cac and cac(2) shifted with increasing polyion charge density. Bulk studies have shown that the cac decreases with increasing charge density of the polyion (43). Accordingly, the binding of the surfactant, seen as an increase in the adsorbed amount, starts at lower concentrations for the highly charged cat-HEC(1.1); see Figure 5a.

Quantitative Differences between cat-guar/Surfactant and cat-HEC/Surfactant Mixtures. The phase studies, gel-swelling, and adsorption experiments all demonstrate a qualitatively similar behavior for cat-guar and cat-HEC in their mixtures with anionic surfactants, but there are important quantitative differences. The phase studies reveal that mixtures of cat-guar and anionic surfactant have much larger two-phase regions compared to the corresponding mixtures with cat-HEC. The weight ratio of surfactant-to-polyelectrolyte at redissolution was 1.5:1 in cat-guar/SDS mixtures compared to 0.8:1 for cat-HEC/SDS. The amount of adsorbed PI/SI complexes at the adsorption maximum on hydrophilic silica was larger for cat-guar than for cat-HEC. Further, the recharging and redissolution of the PI/SI complexes, observed as a desorption from the surface, as a turbidity drop in the bulk, or as a reswelling of the gel, occurred at a much wider surfactant concentration interval and finished at much higher surfactant concentrations, with cat-guar compared to cat-HEC. The relative difficulty of redissolving complexes of cat-guar by surfactant was noted in early publications of Goddard and Hannan (11) and in the studies of Anthony et al. (23), but our experiments give a much more detailed picture; in particular, they clearly demonstrate the gradual nature of the surfactant binding to cat-guar above the cac(2). How can we understand these differences between the two cationic polysaccharides?

Previous gel-swelling experiments on synthetic polyelectrolyte gels suggest that a cooperative excess binding of surfactant (above charge equivalence), of a magnitude sufficient to result in a redissolution, will only occur if there is a hydrophobic interaction between the surfactant and polyion in addition to the electrostatic attraction (10). An increasing strength of this hydrophobic interaction will decrease the value of the cac(2) and increase the extent of excess surfactant binding. We therefore suggest that the differences between cat-guar and cat-HEC can be explained by a weaker hydrophobic interaction between the surfactant and cat-

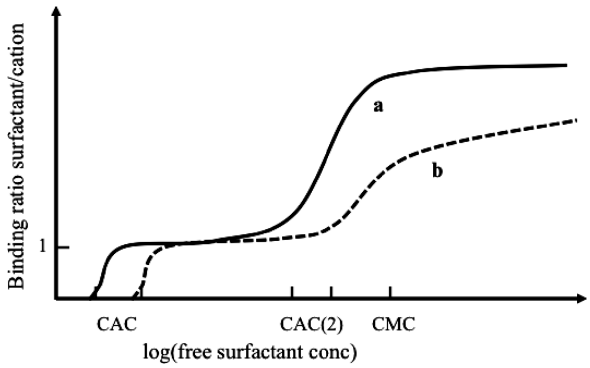

FIGURE 10. Schematic picture of surfactant binding isotherms in mixtures of hydrophobic polycation and anionic surfactant. The diagram shows the PI:SI ratio in the complex as a function of the free-surfactant concentration in the bulk: (a, full line) more hydrophobic polycation; (b, dashed line) less hydrophobic polycation. See the text for details.

guar, consistent with the less hydrophobic character of this polyion that was inferred from the adsorption measurement on hydrophobic silica (Figure 3).

The schematic binding isotherm in Figure 10 illustrates the expected differences in the binding of anionic surfactant to cationic polymers that differ in hydrophobicity. The more hydrophobic polyion (part a), which here corresponds to cat-HEC, has a low cac. The excess binding of the surfactant, commencing at the cac(2), is sufficiently strong to saturate the neutral PI/SI complex at a free-surfactant concentration already slightly below the surfactant cmc (9). The redissolution of the complex may thus appear at concentrations slightly below the surfactant cmc. The less hydrophobic polyion (part b), here corresponding to cat-guar, gives a high cac and shows a weaker and more gradual surfactant binding above a higher cac(2). The binding has therefore not reached saturation at the surfactant cmc but continues as the surfactant concentration increases past the cmc. However, the surfactant activity increases very slowly with increasing concentration beyond cmc. Therefore, the continued surfactant binding becomes very gradual. Such a continued gradual surfactant binding above the cmc has previously been inferred for certain weakly interacting pairs of neutral polymer and ionic surfactant from gel-swelling experiments (44). Evidently, this additional binding can eventually give rise to a redissolution of the PI/SI complex at some free-surfactant concentration far above the cmc.

The gel-swelling experiments (see Figure 9; similar results for SLE3S are available as the Supporting Information) give support to the differing hydrophobicities of cat-HEC and cat-guar and the correspondingly different features of the surfactant binding isotherms. The initial collapse part of the gel-swelling isotherm is much more gradual, and the minimum in the gel volume is reached later for the cat-guar gels than for the cat-HEC gels, indicating a weaker interaction of the surfactants with cat-guar. The reswelling of the cat-guar gels occurs gradually over a large surfactant concentration interval, compared to the rather abrupt reswelling of the cat-HEC gels. The surfactant cmc is reached before the cat-guar polyion is saturated with surfactant. Then, the binding continues past the cmc but necessarily becomes much more gradual, as pointed out above. Indeed, Anthony et al. also concluded that free micelles are always present before there is a complete redissolution of cat-guar with alkyl sulfates (23).

Although much work has been spent on modeling the binding of charged surfactants to oppositely charged polymers (45, 46), very few studies address the situation that is of most interest in the present work, that is, the redissolution phenomenon occurring at an excess of surfactant. Notable exceptions are the recent simulation works of Linse and coworkers, showing that a redissolution of linear PI (47), and a reswelling of polyelectrolyte gels (48), occurs in systems containing an excess of oppositely charged "macroions", mimicking surfactant micelles. However, these simulations did not treat the case of special concern here, where there is an additional (hydrophobic) attraction between the PI and macroions.

CONCLUSIONS

The combination of phase studies, turbidity measurements, gel swelling, DLS, and in situ ellipsometry gives a detailed picture of the relationship between bulk and surface properties of oppositely charged PI/SI mixtures and of the molecular events governing these properties. All experiments demonstrate the precipitation—redissolution behavior of a PI/SI complex that occurs upon increasing the surfactant concentration. There is a close correspondence between the adsorption maximum obtained in the surfactant titration experiments from dilute solutions and the bulk turbidity maximum observed in the same solutions. This is because both surface adsorption and bulk phase separation are consequences of the interaction of the surfactant with the polyion. This means that simple turbidity experiments can serve as useful guides to the adsorption behavior of PI/SI complexes at a surface. More detailed information on the surfactant binding isotherm can be gained from gel-swelling experiments: quantitative information on the cac and cac(2) and qualitative information on the extent and cooperativity of the binding steps commencing at the two cac's.

Changing the charge density of cat-HEC gives rise to a shift in the cac's, whereas the shift in the redissolution phase boundary is insignificant. cat-HECs of different charge densities showed that a high turbidity in the bulk does not necessarily imply a high level of adsorption to a hydrophilic surface. In fact, the relationship was the opposite for the investigated polyelectrolyte/surfactant pairs.

cat-guar and cat-HEC show qualitatively similar behavior in mixtures with anionic surfactant, but there are quantitative differences. We propose that these differences can be understood in terms of differences in the hydrophobicity of the PI. It is easier to dissolve a cat-HEC/surfactant complex by excess surfactant, compared to a cat-guar/surfactant complex, because of a stronger hydrophobic interaction between cat-HEC and the surfactant. For the investigated anionic surfactants, the hydrophobic interaction with cat-guar is so weak that the polyion is not saturated with surfactant when the free-surfactant concentration reaches the cmc. The binding continues past the cmc, and some of this additional binding is required in order to reach a

complete redissolution of the cat-guar/surfactant complex. This leads to the unusually wide precipitation region for cat-guar that was observed previously but not explained. The width of the phase separation region has important consequences for the deposition of PI/SI complexes by dilution, as in a rinsing process, as we have found in studies to be published separately.

The results on cat-guar and cat-HEC imply that, in oppositely charged PI/SI mixtures, the hydrophobicity of the polyion can be used to tune the range of surfactant concentrations where both a phase separation and a peak in the surface adsorption occur. This important conclusion has been confirmed by the results in our laboratory, to be published separately, from experiments on synthetic model PI.

The choice of surfactant is also important to control and tune the redissolution behavior of PI/SI mixtures. In dilute solutions, it is the tendency of the surfactant to self-associate in micelles, as reflected by its cmc and cac values, that determines the phase diagram. At higher polyion concentrations, any polydispersity of the surfactant component should also play a role.

Acknowledgment. Alexandra Andersson, Biochemistry Department, Lund University, is gratefully acknowledged for the investigation of the protein content in the cat-guars by BCA assay. Karin Schillén and David Löf, Division of Physical Chemistry, Lund University, are gratefully acknowledged for valuable discussions and assistance during the DLS experiments. Ronita Marple, Beauty Analytical, Procter & Gamble, is gratefully acknowledged for GPC-LS analysis of the PI. Björn Lindman, Division of Physical Chemistry, Lund University, is gratefully acknowledged for insightful discussions during the project and valuable comments to the manuscript. This study was supported by funds from Procter & Gamble (to A.V.S.) and the Swedish Research Council (to T.N. and L.P.).

Supporting Information Available: Discussions on the purification procedures of cat-guar, including the results on adsorption and turbidity of unpurified cat-guar, and results and discussions regarding SLE3S, that is, ellipsometry, turbidity, phase separation, and gel-swelling experiments, for mixtures of cat-guar and cat-HEC(0.6) with SLE3S. This material is available free of charge via the Internet at http://pubs.acs.org.

REFERENCES AND NOTES

(1) Rodriguez, R.; Alvarez-Lorenzo, C.; Concheiro, A.; Eu., J. *Pharm. Sci.* **2003**, *20*, 429–438.
(2) Bronich, T. K.; Nehls, A.; Eisenberg, A.; Kabanov, V. A.; Kabanov, A. V. *Colloids Surf. B* **1999**, *16*, 243–251.
(3) Marchioretto, S.; Blakely, J. *SOFW J.* **1997**, *123*, 811–812, 814-816, 818.
(4) Axberg, C.; Wennerburg, A. M.; Stenius, P. *Prog. Water Technol.* **1980**, *12*, 371–384.
(5) Thalberg, K.; Lindman, B. Polymer–surfactant interactions—recent developments. In *Interactions of Surfactants with Polymers and Proteins*; Goddard, E. D., Ananthapadmanabhan, K. P., Eds.; CRC Press: Boca Raton, FL, 1993; p 203.
(6) Piculell, L.; Lindman, B.; Karlström, G. Phase behavior of polymer–surfactant systems. In *Polymer–Surfactant Systems*; Kwak, J. C. T., Ed.; Marcel Dekker: New York, 1998; Chapter *3*, pp 65—141.
(7) Goddard, E. D. *Colloids Surf.* **1986**, *19*, 301–329.
(8) Kwak, J. C. T. *Polymer–Surfactant Systems*; Marcel Dekker, Inc.: New York, 1998.
(9) Sjöström, J.; Piculell, L. *Colloids Surf. A* **2001**, *183–185*, 429–448.
(10) Lynch, I.; Sjöström, J.; Piculell, L. *J. Phys. Chem. B* **2005**, *109*, 4258–4262.
(11) Goddard, E. D.; Hannan, R. B. *J. Am. Oil Chem. Soc.* **1977**, *54*, 561–566.
(12) Ananthapadmanaban, K. P.; Leung, P. S.; Goddard, E. D. *Colloids Surf.* **1985**, *13*, 63–72.
(13) Thalberg, K.; Lindman, B.; Bergfeldt, K. *Langmuir* **1991**, *7*, 2893–2898.
(14) Carnali, J. *Langmuir* **1993**, *9*, 2933–2941.
(15) Hiwatari, Y.; Yoshida, K.; Akutsu, T.; Yabu, M.; Iwai, S. *Int. J. Cosmet. Sci.* **2004**, *26*, 316.
(16) Claesson, P. M.; Dedinaite, A.; Meszaros, R.; Varga, I. *Colloids Interface Sci. Ser.* **2007**, *3* (Colloid Stability and Application in Pharmacy), 337–395.
(17) Dedinaite, A.; Claesson, P.; Bergström, M. *Langmuir* **2000**, *16*, 5257–5266.
(18) Rojas, O. J.; Claesson, P. M.; Berglund, K. D.; Tilton, R. *Langmuir* **2004**, *20*, 3221–3230.
(19) Berglund, K. D.; Przybycien, T. M.; Tilton, R. D. *Langmuir* **2003**, *19*, 2705–2713.
(20) Braem, A. D.; Biggs, S.; Prieve, D. C.; Tilton, R. D. *Langmuir* **2003**, *19*, 2714–2721.
(21) Penfold, J.; Tucker, I.; Staples, E.; Thomas, R. K. *Langmuir* **2004**, *20*, 7117–7182.
(22) Penfold, J.; Tucker, I.; Thomas, R. K. *Langmuir* **2005**, *21*, 11757–11764.
(23) Anthony, O.; Marques, C. M.; Richetti, P. *Langmuir* **1998**, *14*, 6086–6095.
(24) Voisin, D.; Vincent, B. *Adv. Colloid Interface Sci.* **2003**, *106*, 1–22.
(25) Gruber, J. V.; Lamoureux, B. R.; Joshi, N.; Moral, L. *Colloids Surf. B* **2000**, *19*, 127–135.
(26) Gruber, J. V.; Lamoureux, B. R.; Joshi, N.; Moral, L. *J. Cosmet. Sci.* **2001**, *52*, 131–136.
(27) Ohbu, K.; Hiraishi, O.; Kashiwa, I. *J. Am. Oil Chem. Soc.* **1982**, *59*, 108.
(28) Drovetskaya, T. V.; Kreeger, R. L.; Amos, J. L.; Davis, C. B.; Zhou, S. *J. Cosmet. Sci.* **2004**, *55*, S195–S205.
(29) Terada, E.; Samoshina, Y.; Nylander, T.; Lindman, B. *Langmuir* **2004**, *20*, 1753–1762.
(30) Terada, E.; Samoshina, Y.; Nylander, T.; Lindman, B. *Langmuir* **2004**, *20*, 6692–6701.
(31) Svensson, A.; Sjöström, J.; Scheel, T.; Piculell, L. *Colloids Surf. A* **2003**, *228*, 91–106.
(32) Miyake, M.; Kakizawa, Y. *Colloid Polym. Sci.* **2002**, *280*, 18–23.
(33) Shubin, V.; Petrov, P.; Lindman, B. *Colloid Polym. Sci.* **1994**, *272*, 1590–1601.
(34) Shubin, V. *Langmuir* **1994**, *10*, 1093–1100.
(35) Seaman, J. K. In *Handbook of Water-Soluble Gums and Resins*; Davidson, R. L., Ed.; McGraw-Hill: New York, 1980; Chapter 6.
(36) Mukerjee, P.; Mysels, K. J. *Critical Micelle Concentrations of Aqueous Surfactant Systems*; National Bureau of Standards: Washington, DC, 1971.
(37) Tokiwa, F. *J. Phys. Chem.* **1968**, *72*, 1214–1217.
(38) Tiberg, F.; Landgren, M. *Langmuir* **1993**, *9*, 927–931.
(39) Jansson, J.; Schillén, K.; Olofsson, G.; Cardoso da Silva, R.; Loh, W. *J. Phys. Chem. B* **2004**, *108*, 82–92.
(40) Guillemet, F.; Piculell, L. *J. Phys. Chem.* **1995**, *99*, 9201–9209.
(41) Zimin, D.; Craig, V. S. J.; Kunz, W. *Langmuir* **2004**, *20*, 2282–2291.
(42) Rojas, O. J.; Ernstsson, M.; Neuman, R. D.; Claesson, P. M. *Langmuir* **2002**, *18*, 1604–1612.
(43) Hansson, P.; Almgren, M. *J. Phys. Chem.* **1996**, *100*, 9038–9046.
(44) Lynch, I.; Sjöström, J.; Piculell, L. *J. Phys. Chem. B* **2005**, *109*, 4252–4257.
(45) Linse, P., Piculell, L.; Hansson, P. Models of polymer–surfactant complexation. In *Polymer–Surfactant Systems*; Kwak, J. C. T., Ed.; Marcel Dekker: New York, 1998; pp 193—238.
(46) Shirahama, K. The nature of polymer–surfactant interactions. In *Polymer–Surfactant Systems*; Kwak, J. C. T., Ed.; Marcel Dekker: New York, 1998; pp 143—191.
(47) Skepö, M.; Linse, P. *Macromolecules* **2003**, *36* (2), 508–519.
(48) Edgecombe, S.; Linse, P. *Langmuir* **2006**, *22* (8), 3836–3843.

AM900378B